Solid State Properties of Thin Films of New Copoly(azomethine-sulfone)s

Luminita Marin,[1] Daniel Timpu,[1] Vasile Cozan,[1] Gheorghe I. Rusu,[2] Anton Airinei[1]

[1]*"Petru Poni" Institute of Macromolecular Chemistry, Iasi, Romania*
[2]*Faculty of Physics, "Al.I.Cuza" University, Iasi, Romania*

Received 15 April 2010; accepted 29 August 2010
DOI 10.1002/app.33313
Published online 1 December 2010 in Wiley Online Library (wileyonlinelibrary.com).

ABSTRACT: A series of four copoly(azomethine-sulfone)s have been synthesized and extensively characterized. The chemical design has been thought to obtain semiconducting properties and thermotropic behavior matching the processing of the materials from the ordered melted state, suitable for the spontaneous alignment of molecules in the active layer on a substrate. Prototypes of thin films based on this series of polymers have been electrically and structurally characterized. It was found that the respective polymers show typical semiconducting properties. The thermal properties with particular reference to their mesomorphic state were checked by using differential scanning calorimetry, polarized light microscopy, and thermogravimetric analysis techniques. Morphological characterization was realized by atomic force microscopy and X-ray diffraction measurements. Some correlations between electrical properties and packing closeness were established. © 2010 Wiley Periodicals, Inc. J Appl Polym Sci 120: 1720–1728, 2011

Key words: polyimines; mesomorphism; charge transport; morphology; atomic force microscopy

INTRODUCTION

Aromatic polyazomethines are a well known class of polymers having thermal stability, liquid crystalline behavior, semiconducting and optical properties, environmental stability, etc.[1] Among the semiconducting polymers, the polyazomethine derivatives are further advantageous, because they can be both p- and n-doped, resulting in a polymer with mutual hole and electron charge carrier properties.[2] This aspect is highly sought for reducing the number of layers required for functional devices and is not readily achievable with current conjugated materials because of the incompatibility of the highest occupied molecular orbital and lowest unoccupied molecular orbital energy levels with currently used electrodes. There are many studies reporting the synthesis of polyazomethines and their electrical properties before and after doping.[3–5] For instance, Kaya et al.[5] showed that, by I_2 doping, the conductivity of perylene-containing polyazomethines improved by about five orders of magnitude.

The main disadvantages of polyazomethines are their insolubility and infusibility, drawbacks which limit their applications because of the low processability. The synthesis of some polyazomethines containing diphenylsulfone units in the main chain demonstrated that the introduction of the sulfone group affords good solubility and accessible melting transitions while the thermal stability, thermotropic behavior, and semiconducting properties are kept.[6] The presence of the mesomorphic state offers the possibility to obtain ordered films from the ordered melt. The self-organization is reasonably expected to facilitate the easy formation of a large area monodomain film or multidomain films with no physical grain boundaries between the small domains, with uniform alignment of molecules through their characteristic orientational order.[7] Such a property is very important for organic semiconductors whose carrier mobility depends on the degree of molecular ordering and connectivity among domains.[8] For example, Van Breemen et al.[9] have reported the formation of highly ordered monodomains of liquid crystalline compounds with better semiconducting properties than multidomain devices.

Here, we report the study of structural, morphological, thermal, and electrical properties of a series of thermotropic copoly(azomethine-sulfone)s whose structure is especially designed to obtain good solubility, accessible melting temperature, liquid crystalline behavior, and electrical properties. The structural and morphological properties of thin semiconducting films of these polymers are monitored to gain a perspective on the importance of the self-organizing nature of such materials.

Correspondence to: L. Marin (lmarin@icmpp.ro).
Contract grant sponsor: CEEX-MATNANTECH; contract grant number: 52/2006.

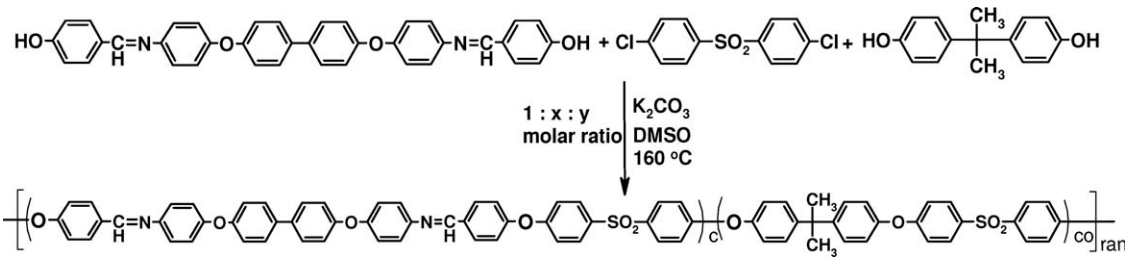

Scheme 1 Synthesis of the P1–P4 polymers.

EXPERIMENTAL

Chemicals and synthesis

Statistic copoly(azomethine-sulfone)s have been prepared by using the classical Williamson condensation reaction between sulfonyl bis(4-chlorophenyl) and two bisphenols: 2,2-bis(4-hydroxyphenyl)propane (bisphenol A) and 4,4′-bis[4-(4-hydroxybenzylideneimino)phenoxy] biphenyl, taken in various molar ratios ($1 : x : y$), as shown in Scheme 1.[6] After water washing, the copolymers were refluxed in methanol for 3 h and hot filtered to extract the soluble oligomers, to reduce the polydispersity index and, by consequence, to improve their properties.

The polymers under investigation were studied on thin films samples deposited from dimethylformamide (DMF) solutions onto glass substrates. The thermal treated films were obtained by two heating–cooling scans, the upper temperature being situated before the onset of thermal degradation.

Instrumentation

Infrared (IR) spectra were recorded on a Fourier transform IR (FT-IR) Bruker Vertex 70 Spectrophotometer in transmission mode, by using KBr pellets. Molecular weight distributions of polymers were measured by gel permeation chromatography (GPC) analysis carried out on a PL-EMD 950 Evaporative Light Scattering Detector instrument, using DMF as eluent and standard polystyrene samples for calibration.

The differential scanning calorimetry (DSC) measurements were carried out by using a Mettler TA Instrument DSC 12E at a heating/cooling rate of 10°C min^{-1} under nitrogen atmosphere; the transition temperature was read at the top of the peak.

The mesophases of polymers have been studied by observation of the textures with an Olympus BH-2 polarized light microscope equipped with a THMS 600/HSF9I hot stage, under cross polarizers.

Thermogravimetric analysis (TGA) was carried out by using a MOM Q Derivatograph, Hungary, at a heating rate of 10°C min^{-1}, in air. Wide-angle X-ray diffraction (XRD) measurements were performed at room temperature using a modernized DRON 2.0 Diffractometer, CoKα radiation, λ = 1.79019 Å, 30 kV, 10 mA.

Atomic force microscopy (AFM) images were collected in semicontact mode with a Solver PRO-M, NT-MDT, Russia. The temperature dependence of the electrical conductivity was investigated using surface type cells.[10] Thin indium films were used as electrodes. The thickness of polymeric films was determined by Fizeau's method for fringes of equal thickness, using an interferential microscope MII-4.

RESULTS AND DISCUSSIONS

Copolymers P1–P4 having the structure shown in Scheme 1 have been prepared by Williamson etherification reaction of sulfonyl bis(4-chlorophenyl) with a mixture of mesogenic bisphenol (4,4′-bis[4-(4-hydroxybenzylideneimino) phenoxy]biphenyl) and bisphenol A taken in various molar ratios (Table I), by using dimethylsulfoxide as solvent. The resulting polymers were isolated by precipitation in water, followed by washing in water to remove the solvent and inorganic salts, refluxing in methanol to remove the oligomers and drying.

The chemical structure of these polymers was identified by FTIR spectra and elemental analysis. All the FTIR spectra exhibited characteristic adsorption bands at 1640–1625 cm^{-1} due to the —CH=N— stretching, at 1335–1300 cm^{-1} and 1160–1150 cm^{-1} due to the asymmetric and symmetric stretching of —SO_2— group, and 1255–1245 cm^{-1} due to the —O— stretching. The CH_3 groups from bisphenol A were evidenced by absorption peaks at 2990–2950 and 2895–2860 cm^{-1}. The broad absorption peaks at 3090–3030 cm^{-1} were attributed to C—H aromatic

TABLE I
Molecular Weight Measurements of the Polymers P1–P4

Polymer code	$x : y$[a]	M_w	M_n	M_w/M_n
P1	1 : 0	31,103	11,685	2.66
P2	0.75 : 0.25	7,245	6,300	1.15
P3	0.50 : 0.50	8,110	6,540	1.24
P4	0.25 : 0.75	9,028	7,400	1.22

[a] $x : y$ represents mesogenic bisphenol : bisphenol A molar ratio in polycondensation reaction.

bonds, whereas the strong absorption peaks from 1600 to 1585, 1500, and 1485 were assigned to aromatic C=C bonds. Elemental analysis data showed a good concordance between the calculated and experimental values of percentage weight for both nitrogen and sulfide content.

The molecular weights of copolyazomethines P1–P4 were measured by GPC, by using polystyrene standards. The molecular weight values M_w are in the range 32,000–7,245, M_n in the range 11,600–6,300, and polydispersity M_w/M_n in the range of 1.15–2.66 (Table I). It should be noted that GPC measurements by using polystyrene standards only provide a crude estimate of molecular weights and not an accurate evaluation. But these values of molecular weight can be used for comparison. As can be seen in Table I, the present polymers have fairly good values of molecular weight and narrow molecular weight distribution, comparable with that of other aromatic polyazomethines.[11]

The solubility tests were carried out in different solvents by using 10 mg sample and 10 mL solvent. All the polymers were soluble in polar amidic solvents as *N*-methylpyrrolidinone, DMF, and dimethylacetamide and partially soluble in less polar liquids, like pyridine or tetrahydrofuran. The improved solubility of these polymers compared with conventional aromatic polyazomethines, which are only soluble in strong acids such as H_2SO_4 and methanesulfonic acid, can be explained by the bending of the chains at sulfur and carbon (with sp^3 hybridization) atoms, which makes the shape of the macromolecules to be far from a "rigid rod," and thus facilitates the diffusion of the small molecules of solvent. Moreover, the copolymerization process rendered more solubility

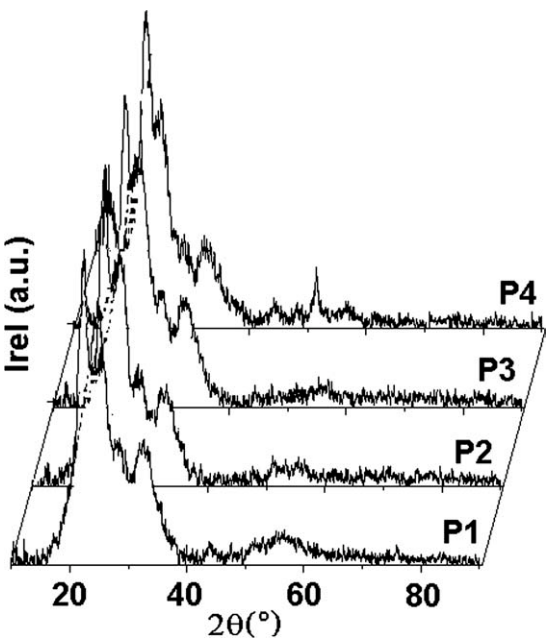

Figure 1 Wide-angle XRD of the polymers P1–P4.

TABLE II
The *d*-Spacing Corresponding to the Diffraction Peaks Observed in the X-ray Diffraction Patterns of the Studied Poly(azomethine-sulfone)s

P1 (χ = 22%)		P2 (χ = 30%)		P3 (χ = 25%)		P4 (χ = 24%)	
2θ	*d* (Å)	2θ	*d* (Å)	2θ	*d* (Å)	2θ	*D* (Å)
22.30	4.56	22.21	4.79	22.19	4.59	22.35	4.55
24.83	4.11	25.01	4.08	24.86	4.11	24.96	4.09
28.52	3.59	28.25	3.63	28.70	3.57		
32.72	3.15	33.12	3.11	32.70	3.15	32.16	3.20

to the present copolymers compared with classical aromatic polyazomethines.[1,12]

To investigate the structure of P1–P4 polymers, X-ray diffractograms for powder samples were recorded (Fig. 1). Their XRD patterns contain some intensive peaks, situated above of amorphous halo; the sharp bands correspond to crystalline (orderly) regions and broad halo refer to amorphous (nonorderly) regions. These XRD patterns indicate the presence of what we define as semicrystalline state that was formed during solution polycondensation.

Percentage of crystallinity was measured as ratio of crystalline area to total area. The degree of crystallinity (χ) of all studied copolymers was in the range 20–30% (Table II) and could be explained by the segregation of homopolymer sequences, which occur by chance within the macromolecules. It can be remarked that the highest value of crystallinity degree is obtained for P2 polymer whose polydispersity index value is the smallest (M_w/M_n: 1.15), and its content of mesogenic units is higher than P3 and P4 polymers (M_w/M_n: 1.22 and 1.24). Despite the fact that P1 has the highest content of mesogenic groups in its macromolecular chains, its large polydispersity (M_w/M_n: 2.66) hinders the self-assembling of the mesogenic groups, and the polymer has the smallest degree of crystallinity.

The *d*-spacing, calculated with Bragg's law by using the measured diffraction angle in the XRD patterns, for all the polymers are enclosed in Table II. The *d*-spacing calculated for the Bragg reflections corresponding to the interchain distances is in the range 4.79–3.11 Å (Table II). The relatively close contact of the azomethinic mesogenic units may lead to the good charge conduction, which will be discussed below. The different *d*-spacing values reflect various intensities of interchains forces because of the different kinking units, which disrupt the linearity of the macromolecular chains.

Thermal properties

Because small amounts of thermally decomposed material drastically affect the thermotropic behavior,

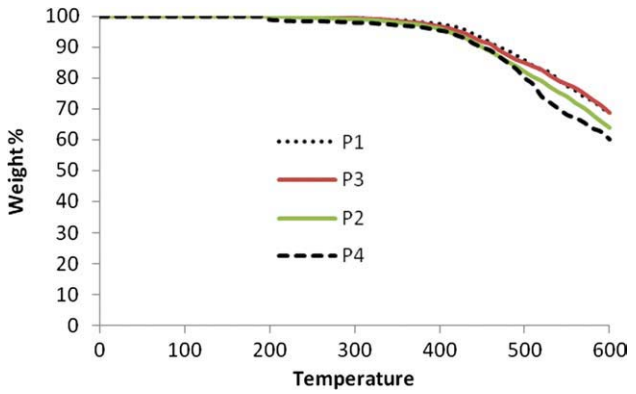

Figure 2 TGA traces of P1–P4 copolymers. [Color figure can be viewed in the online issue, which is available at wileyonlinelibrary.com.]

we evaluated the thermal stability by TGA, considering the onset of thermal decomposition, i.e., the temperature corresponding to initial 1% of weight loss ($T_{1\%}$). TGA thermograms were measured at a heating rate of 12°C min^{-1}, in air. Figure 2 shows representative plots of weight residue (wt %) versus temperature, up to 600°C. The polymers exhibit high thermal stability, with similar behavior during the degradation process: a slight decomposition started above 200°C but with 1% weight loss up to 330°C; the 10% weight loss appeared at temperatures above 450°C (Table III). The degradation residues of the examined polymers at 600°C are rather high, about 60% in air. All these data indicate very good thermal stability for the studied polymers.

The DSC thermograms of the polymers P1–P4 have been recorded during a heating–cooling–heating cycle at a heating rate of 10°C min^{-1}. All four polymer samples exhibit two small, broad endothermic peaks in the first heating scan (first-order transitions) and only a single trace inflection corresponding to glass transition (second-order transition, T_g) in the cooling and second heating scan. By correlating of DSC and polarized light microscopy (POM) data, the first endothermic peak was attributed to the melting process (T_m = melting temperature) and the second one to the isotropization (T_i = isotropization temperature). The temperature values corresponding to these transitions are enclosed in Table III. The values of glass-transition temperatures (T_g) of the polymers P1–P4 are in the range 114–134°C, being lower than those of related polyazomethines without diphenylsulfone and bisphenol A units.[11] Such behavior could be attributed to the higher free volume determined by the presence of kinked groups. Moreover, these copolymers show melting points between 184°C and 284°C, compared with related polyazomethines that do not melt before decomposition. This means that the present polymers could be also processed from the molten state. The small enthalpy changes registered by DSC for both first-order transitions correspond to small changes in the semicrystalline architecture, in agreement with small degree of crystallinity appreciated from X-ray measurements. The thermodynamic data are enclosed in Table III.

The POM was performed to clarify the polymers behavior in the DSC measurements. Corresponding to the first endotherm, in POM, we observed the appearance under shear of a birefringent viscous fluid, for all the samples (Fig. 3). The viscosity decreased when the temperature increased, and the sample flows at higher temperature (Table III). The textures are fine, often shown by the thermotropic polymers based on stiff chains without flexible spacers.[12,13] The second broad endothermic peaks correspond to the slow isotropization because of the interchain forces by variable intensity. On cooling, the mesophase did not appear from the isotropic liquid.

The formation of a mesophase in the first heating scan for the studied polymers could be explained by the preformed arrangement of the macromolecules in a semicrystalline state. During the first transition, the macromolecules gain thermal energy, and, thus, the conformational disorder of the single tetrahedrally coordinated C and S atoms increases, but the ordered structure is maintained because of the strong attractive π-interactions between the aromatic cores; the mesophase state is the result of two antagonistic features: attractive interchain forces and

TABLE III
Thermodynamic Data of P1–P4

	DSC transition temperatures in °C (enthalpy changes in J g^{-1})			POM transition temperatures in °C		TGA	
Code	T_g	T_m (ΔH)	T_i (ΔH)	T_m[a]	T_i[b]	T_1	T_{10}
P1	127	284 (3.38)	302 (2.04)	287	305	330	470
P2	125	210 (5.67)	261 (3.9)	225	258	330	465
P3	134	205 (12.5)	259 (4.6)	218	260	300	450
P4	114	184 (9.8)	237 (4.2)	194	230	200	450

[a] The temperature corresponding to the birefringence sample flowing.
[b] The temperature corresponding to the beginning of isotropization.

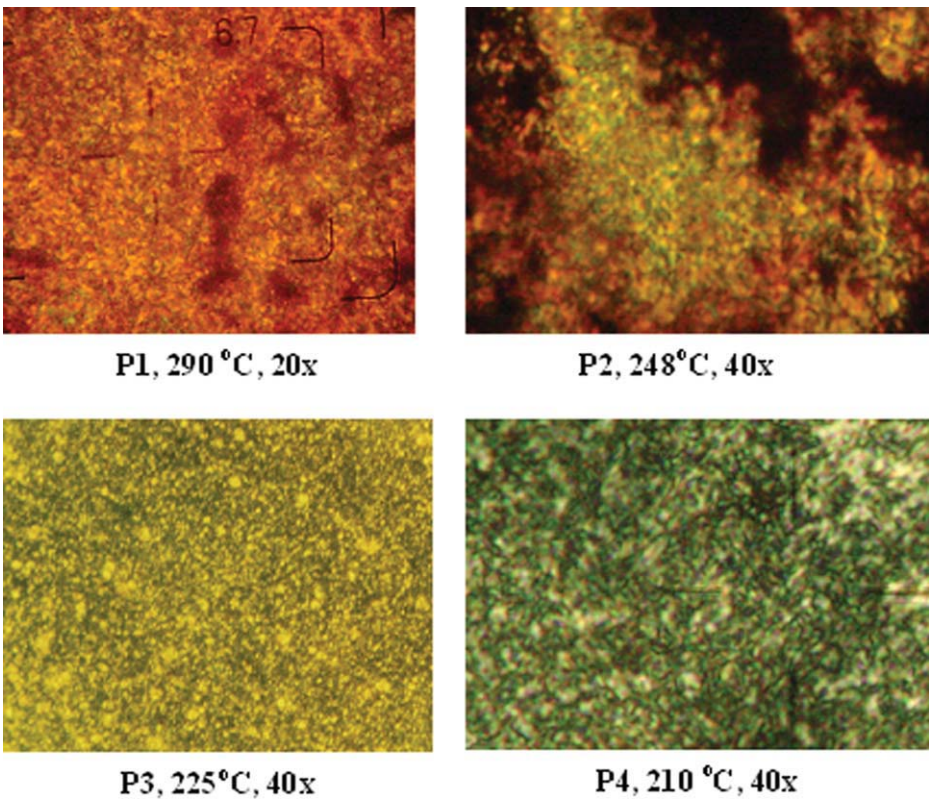

Figure 3 Polarized optical micrographs of the P1–P4 copolymers, in the first heating. [Color figure can be viewed in the online issue, which is available at wileyonlinelibrary.com.]

conformational disorder. During the cooling scan, the rigid macromolecules have enough energy to move in the isotropic state, but in the absence of a flexible spacer, the self-assembling does not act, and the macromolecules freeze in disordered state. Nevertheless, the birefringent viscous fluid, which appears between the semicrystalline solid and the isotropic liquid state on increasing the temperature in the first heating scan, corresponds to a ordered molten, and this behavior brings about new processing opportunities.[9,14,15] Taking into account the XRD, DSC, and POM measurements data, it seems reasonable to assume that these polymers form a plastic mesophase.[13,16]

Semiconducting properties

The electrical conductivity of the synthesized copolymers was measured on thin films deposited on the glass substrates from DMF solutions.[17] To obtain polymeric films with stable structures, the samples, after preparation, were successively heated and cooled within a temperature range, corresponding to their thermal stability (Table IV). The polyethersulfone is considered an insulator, having electrical conductivity about 10^{-16} (Ω^{-1} cm^{-1}), whereas the studied poly(azomethine-sulfone)s showed semiconducting properties with electrical conductivity of 10^{-7} to 10^{-8} (Ω^{-1} cm^{-1}). The higher conductivity can be ascribed to the azomethinic mesogenic cores, which self-assemble in crystalline domains, with a close contact of the mesogenic π-systems and thus good charge conduction (see X-ray discussions). It is observed that the best conductivity is obtained for P2 polymer film, which shows the highest degree of crystallinity. Moreover, it was observed that polymeric films, after the thermal treatment, have a better electrical conductivity than the untreated polymeric films (Table IV). It is known that the granular structure of the films (the grains size and shape, as well as the characteristics of the contact between them) plays an important role in the electronic transfer mechanism of the polymers.[18] For granular (polycrystalline) films, the electronic transport mechanism was based on the consideration that the grain boundaries have an inherent space charge region due to the interface. Consequently, potential barriers to electronic transport result. Heating of the polymeric film modifies its structural characteristics (grain size and shape, concentration of structural defects, properties of intergrain boundaries, etc.) and film purity (removal of the absorbed or/and adsorbed gases, residual solvent from the film casting process, and also accidental impurities introduced during polymer synthesis and the preparation of thin-film samples).[19] To

TABLE IV
Semiconducting Properties of P1–P4

Sample code	d (μm)[a]	T_{max} (°C)[b]	σ_N (Ω^{-1} cm^{-1})[c]	σ_T (Ω^{-1} cm^{-1})[d]	R.E.$_N$[e] (R_{max})	R.E.$_T$[f] (R_{max})
P1	1.84	210	0.11 E-7	8.15 E-7	1.29 (100)	0.196 (10)
P2	1.58	225	0.46 E-7	2.5 E-7	1.17 (80)	0.114 (12)
P3	1.05	215	0.12 E-7	0.81 E-7	7.28 (600)	6.29 (400)
P4	0.38	205	0.024 E-7	0.768 E-7	9.67 (600)	3.52 (300)

[a] Film thickness.
[b] The upper temperature of the thermal treatment.
[c] Electrical conductivity at room temperature.
[d] Electrical conductivity after heat treatment.
[e] Roughness exponent and maximum roughness of the untreated films.
[f] Roughness exponent and maximum roughness of the treated films.

see how the film morphology is influenced by the thermal treatment, polarized optical microscopy and AFM measurements of the studied untreated and treated films were performed. The trial to monitor the degree of crystallinity of the untreated and treated films by X-ray measurements collapsed because the films are very thin compared with the glass substrate thickness, and the obtained X-ray pattern belong, in fact, to the amorphous glass.

Structural studies

The ordered structure of the treated and untreated films has been evidenced by POM. POM images of the untreated films display week birefringence, indicating an ordering degree, confirmed by XRD measurement (Table II). For the treated film of P1 polymer, a strong birefringence was observed, whereas the thermal treated films of P2, P3, and P4 polymers exhibit an isotropic state despite the fact that all the films were treated into the liquid crystalline stability range. The explanation for this behavior is that thin films of samples have lower transition temperatures than thick ones how usually can be observed in POM.[15] These observations indicated that the P1 film, after thermal treatment, was obtained in liquid crystalline state, whereas P2, P3, and P4 films were obtained in isotropic state.

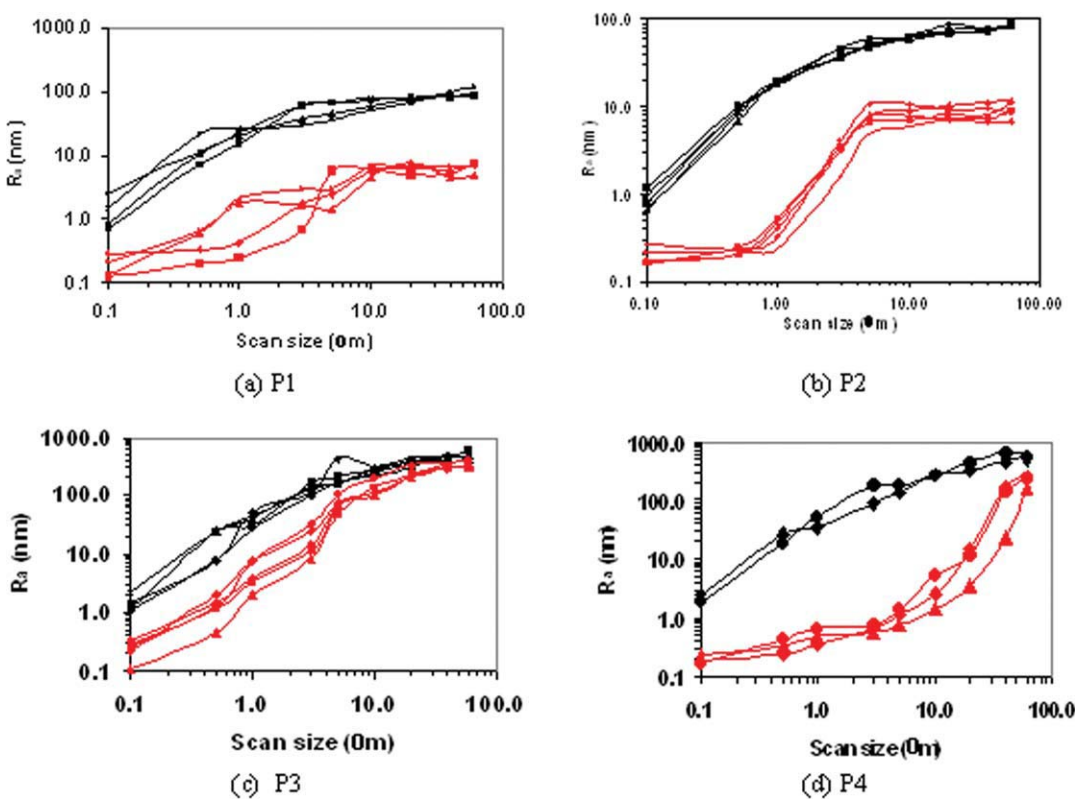

Figure 4 Roughness versus scan size of untreated (black lines) and treated (red lines) P1 (a), P2 (b), P3 (c), and P4 (d) films. [Color figure can be viewed in the online issue, which is available at wileyonlinelibrary.com.]

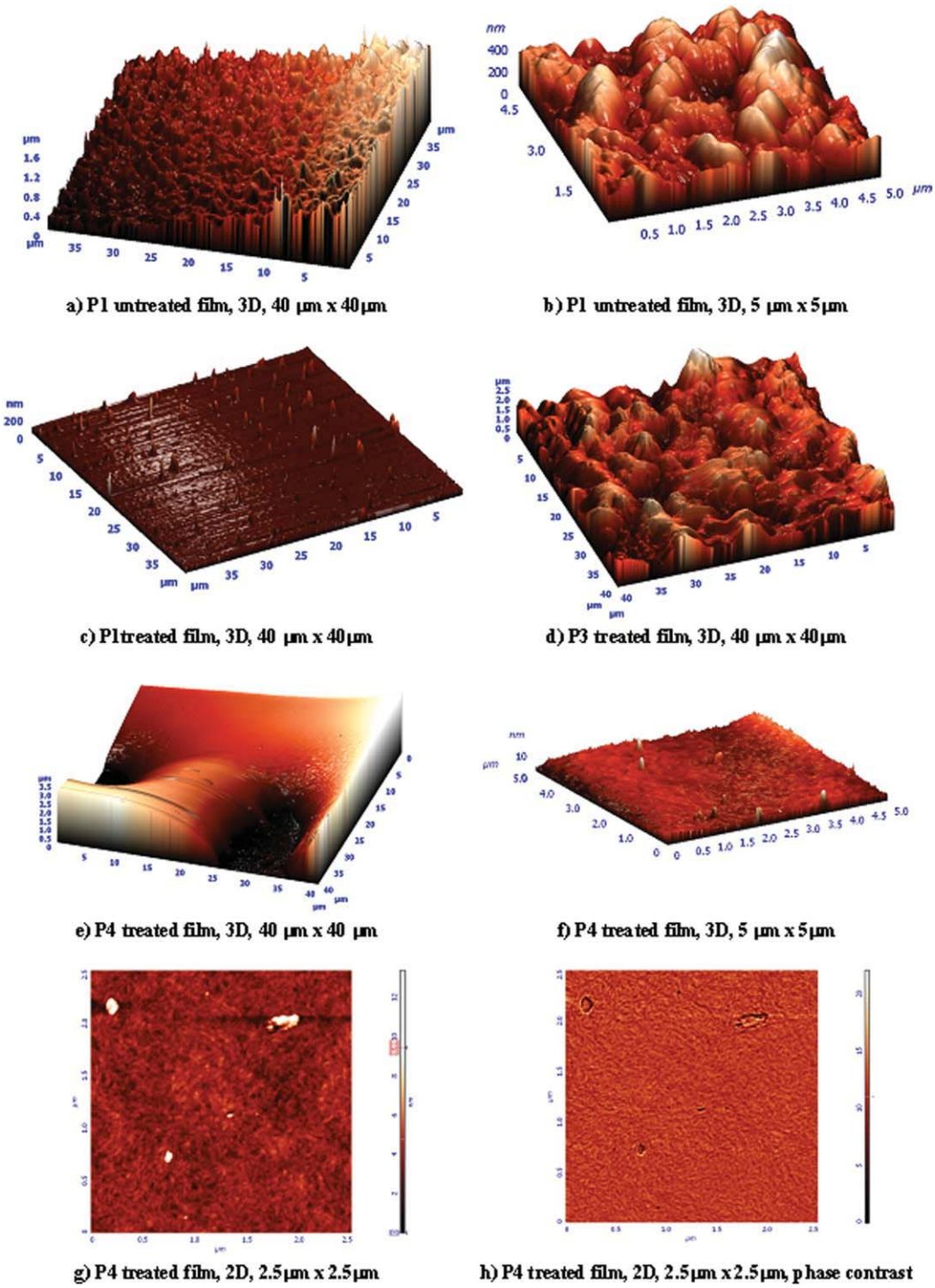

Figure 5 Three-dimensional and two-dimensional topography images of untreated and treated films. [Color figure can be viewed in the online issue, which is available at wileyonlinelibrary.com.]

Morphological characterization

Because of the critical impact of film morphology on electronic device performances,[8,20] the AFM morphological characterization of the treated and untreated film surfaces of the four polymers was considered. Nova v.1443 software was used for recording and analyzing the AFM topographic and phase contrast images. The arithmetic average roughness (R_a) was determined for all explored areas using the definition expressed by:

$$R_a = \frac{1}{n}\sum_{i=1}^{n}[Z_i]$$

where Z_i is the value of the tip height in each point of the image over a reference baseline ($Z = 0$).

Because it is a statistic investigation, the different areas were not "chosen," only landed the cantilever on surface and registered data for concentric squares, beginning with a scan size of 60 μm (60 × 60 μm^2) and decreasing it progressively up to 0.1 μm (0.1 × 0.1 μm^2). For an accurate comparison of the surface characteristics of all films, we calculated the roughness exponent (R.E.) as the slope of roughness versus scan size, in a double log plot.[21] For the surfaces, such a kind of representation is shown in Figure 4.

The roughness exponent values calculated for all the treated and untreated films and the maximum values of the roughness (R_{max}) are enclosed in Table IV. A small roughness exponent value means that the surface is rather planar, whereas a high R.E. value means that the surface looks more like a volume than an actual surface. The analysis of these data clearly reveal smaller values of R.E. for treated films versus untreated films, especially in the case of the polymers with high content of azomethinic mesogen (P1 and P2).

When the roughness of both untreated and treated P1 and P2 poly(azomethine-sulfone) film samples were measured by AFM, significant differences were obtained for the large scanned areas [Fig. 4(a,b)]. The untreated P1 and P2 films show an increasing roughness until very large scanned areas (from 10 to 60 μm) that present somewhat a plateau, which should correspond to a significant macrostructure [Fig. 5(a,b)], whereas, for the treated P1 and P2 films (especially P2), there is a plateau in the range from 0.1 to 0.5 μm of the scanned area size (corresponding to a microstructure) followed by an increase in the roughness until large scanned areas (from 5÷10 to 60 μm) that present a plateau and, thus, a certain macrostructure [Fig. 5(c)]. It is very clear that the untreated P1 and P2 films have rougher surface at the micro- and macroscale (R_{max} about 100) than the treated P1 and P2 films (R_{max} about 10). P3 and P4 untreated and treated films present increasing values of roughness with scanned area size up to large scanned areas 50–60 μm [Figs. 4(c,d) and 5(d,e)], but the treated P4 film show a plateau in the range 0.1–5 μm, indicating a certain microstructure [Fig. 5(f)]. By phase contrast technique, it was proved that the small "hills" seen on the treated films surfaces are not impurities [Fig. 5(g,h)].

These data could be explained taking into account the content of mesogenic units of the polymers. The P1 polymer containing the biggest amount of mesogenic units form by casting from solution large crystallites [Fig. 5(a,b)]. After thermal treatment, the mesogenic units rearrange into a plastic mesophase, and the film becomes almost continuous because of the high viscosity of the rigid polymer, with rarely clusters attributed to the cybotactic groups [Fig. 5(c)]. The other polymers P3 and P4 containing decreasing amounts of mesogenic units and increasing amounts of kinking units of bisphenol A form, by casting from solution, rougher films (the maximum roughness registered is about 600 nm), and, by thermal treatment, their roughness does not decrease much (the maximum roughness registered is about 400 nm for P3 and 300 nm for P4) [Fig. 4(c,d)]. The explanation for small decrease in the P3 and P4 treated films roughness is given by their higher content of kinking bisphenol A units that lead to the formation of lower viscous molten, which has the tendency to form drops [Fig. 5(e)]. Besides, as proved by the POM measurements, the molten samples are isotropic; thus, the cohesion among the parts of macromolecules does not exist or is very weak.

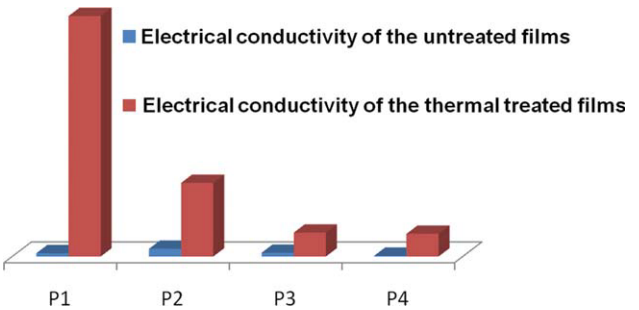

Figure 6 The electrical conductivity of the untreated and treated polymer films. [Color figure can be viewed in the online issue, which is available at wileyonlinelibrary.com.]

By analyzing the AFM, POM, and semiconducting data, some interesting correlations can be established. Thus, by thermal treatment of the polymer films, the surface becomes less rough; fact which can assure a better contact organic material/electrode, and thus better conductivities. Although the P2 polymer film has the best conductivity before thermal treating, the best conductivity after thermal treating was registered for the P1 polymer film; based on the experimental evidence that the difference between the two treated films is the degree of order, we can ascribe its better conductivity to the higher order into plastic mesophase of P1 polymer treated film versus amorphous P2 polymer treated film. For a better view of the data, we represented the polymer conductivities in a graph (Fig. 6).

For P1 sample, whose treated film has an ordered structure in the mesophase state and a homogeneous morphology of the surface, a high increase in the electrical conduction was noticed (about 74 times). For the P2 and P3 samples, whose treated films are amorphous but with a better homogeneity versus untreated films, a slight increase in the electrical conductivity was observed (about six times), whereas P4 sample presents a medium increase in

the electrical conduction (about 32 times). The higher increase in the P4 conductivity treated film versus P2 and P3 could be ascribed to its smaller thickness. We can conclude that ordered films have better charge transport properties than amorphous films, and homogeneity of the amorphous films play an important role in the electronic conduction improving.

CONCLUSIONS

The solid state properties of some new mesomorphic poly(azomethine-sulfone)s were analyzed. The comparative study of the treated and untreated films of these polymers clearly shows the improvement of the charge transport properties of the ordered films versus amorphous films. Also, the amorphous films have better charge transport properties when the film continuity is higher.

References

1. Iwan, A.; Sek, D. Prog Polym Sci 2008, 33, 289.
2. Bourgeaux, M.; Skene, W. G. Macromolecules 2007, 40, 1792.
3. Lee, K.-S.; Won, J. C.; Jung, J. C. Die Makromolekulare Chemie 2003, 190, 1547.
4. Kaya, İ.; Baycan, F.; Doğan, F. J Appl Polym Sci 2009, 112, 1234.
5. Kaya, I.; Koyunce, S.; Culhaoglu, S. Polymer 2008, 49, 703.
6. Marin, L.; Cozan, V.; Bruma, M. Polym Adv Technol 2006, 17, 664.
7. Shimizu, Y.; Oikawa, K.; Nakayama, K.; Guillon, D. Mater Chem 2007, 17, 4223.
8. Taur, Y.; Ning, T. H. Fundamentals of Modern VLSI Devices; Cambridge University Press: New York, 1998.
9. Van Breemen, J. J. M.; Herwig, P. T.; Chlon, C. H. T.; Sweelssen, J.; Schoo, H. F. M.; Setayesh, S.; Hardeman, W. M.; Martin, C. A.; De Leeuw, D. M.; Valeton, J. J. P.; Bastiaansen, C. W. M.; Broer, D. J.; Popa-Merticaru, A. R.; Meskers, S. C. J. J Am Chem Soc 2006, 128, 2336.
10. Rusu, G. I.; Caplanus, I.; Leontie, L.; Airinei, A.; Mardare, D.; Rusu, I. I. Acta Mater 2001, 49, 553.
11. Grigoras, M.; Catanescu, C. O. J Macromol Sci Part C: Polym Rev 2004, 44, 131.
12. Windle, A. H. In Liquid Crystalline and Mesomorphic Polymers; Shibaev, V. P., Lam, L., Eds.; Springer Verlag: New York, 1994; pp 26–76.
13. Damaceanu, M. D.; Marin, L.; Manicke, T.; Bruma, M. Soft Mater 2009, 7, 164.
14. Babacan, V.; Aksoy, S.; Yerlikaya, Z.; Altinok, H. Polym Int 2010, 59, 749.
15. Destri, S.; Porzio, W.; Marin, L.; Damaceanu, M. D.; Bruma, M. J Optoelectr Adv Mater 2007, 9, 1337.
16. Marin, L.; Damaceanu, M. D.; Timpu, D. Soft Mater 2009, 7, 1.
17. Marin, L.; Cozan, V.; Bruma, M. In Proceedings of the 11th European Conference on Organized Films, Potsdam, Germania, July 9–11, 2008; p 47.
18. Seeger, K. Semiconducting Physics, 9th ed.; Springer-Verlag: New York, 2004.
19. Rusu, G. I.; Airinei, A. Rusu;, M.Prepeliţă, P.; Marin, L.; Cozan, V.; Rusu, I. I. Acta Mater 2007, 55, 433.
20. Porzio, W.; Destri, S.; Pasini, M.; Giovanella, U.; Marin, L.; Damaceanu, M. D.; Campione, M. Thin Solid Films 2007, 515, 7318.
21. Macanas, J.; Palacio, L.; Pradanos, P.; Hernandez, A.; Munoz, M. Appl Phys A 2006, 84, 277.